Observability-Index-Based Control Strategy for Induction Machine Sensorless Drive at Low Speed

Gaëtan Lefebvre, Jean-Yves Gauthier, Alaa Hijazi, Xuefang Lin-Shi, Vincent Le Digarcher

Observability-index based control strategy for induction machine sensorless drive at low speed

Gaëtan Lefebvre, *Student Member*, *IEEE*, Jean-Yves Gauthier, Alaa Hijazi, Xuefang Lin-Shi, and Vincent Le Digarcher

***Abstract*—This paper focuses on the observer-based methods for induction machine sensorless drive. It is well known that the use of speed observer is limited at very low stator frequency due to speed unobservability. Some existing methods propose to avoid the zero-stator-frequency working points. These methods are nonetheless limited to high-torque operations. The first contribution of this paper is to analyse finely the speed observability, which leads to the definition of an observability index. The correlation between this index and the observer performance is analysed and illustrated. The second contribution is to propose a control strategy that maximises the observability index and improves the observer performance. The proposed strategy is tested first in open-loop to evaluate the speed observer performance and then in closed-loop to illustrate its pertinence for induction machine sensorless drive. All these results are validated by an experiment. The performed experimentation shows that the proposed control strategy gives better results than the existing method that avoid the zero-frequency working points. It offers a new path for induction machine sensorless drives.**

***Index Terms*—Induction motor drives, Observability, Observation, Sensorless drives**

I. Introduction

FOR more than 30 years, speed-sensorless control of induction machines has taken an important part of the research since it comes at the junction point of industrials expectations and researchers interests. After various speed-observer implementation in the 1990's, for example, adaptive observers [1], extended Kalman filter [2], or extended Luenberger observer [3], the difficulty to use a speed observer for an induction machine near zero-stator-frequency operating conditions has been pointed out in experiments at the beginning of the 2000's [4]. The theoretical study of speed observability of the induction machine has been performed quite simultaneously [5]. It proved that the speed of the induction machine is not observable for zero-stator-frequency operating points. This theoretical limit means that the difficulties to drive the machine will remain whatever the type of observer, the tuning quality and the parameter accuracy. Without fully overcoming this limit, the observer performance can be improved near this limit. For instance, a lot of research has been done on this direction to improve the adaptive full-order observer stability [6] or robustness [7]. It allows to use observer closer to zero-stator frequency operation, but it cannot be a solution for long time operation at very low stator frequency.

In order to overcome this observability theoretical limit, most of the solutions presented in the literature suggest to inject an additional high-frequency (HF) signal to get additional speed information [8], [9]. Such methods generate additional current harmonics and torque oscillation. They are furthermore highly dependant on the machine geometry [10]. So, to reach a good precision on the speed, many injection methods need a finer modelling of the machine [11], [12]. It makes these HF-injection methods uneasy to adapt to any kind of induction machine, and limits their industrial application [13]. Consequently, only few injection methods are used industrially, and a real interest is given to keeping the fundamental model of the induction machine to adapt easily from one machine to another.

Low-frequency signal injection methods [14] are part of these induction machine sensorless drive solutions that keep the fundamental modelling and does not necessitate HF signal injection. This solution, effective for very slowly varying speed, suffers from two drawbacks. The speed observation bandwidth is reported to be around 1 Hz, which makes it difficult to use in closed-loop, and the inertia has to be small since the method relies on the flux position detection through speed oscillation in response to a low torque error [15]. In [16] and [17] is proposed a solution which consists in Avoiding Zero-Frequency (AZF) operating points. This solution improves the performance of the induction machine sensorless drives based on observers. The improvement is nonetheless limited to high-torque operations.

The limitation of these observer-based methods require a deeper study of theirs performance in the neighbourhood of unobservable conditions. Classical observability analysis, as in [5], which gives a binary indicator remains not enough. It is the purpose of this paper in which a continuous measurement of observability is defined to evaluate precisely the observer performance in this neighbourhood. The speed for which the speed becomes unobservable depends on the electrical torque. It always corresponds to regenerative braking conditions. For practical consideration, a delicate area for speed observation is delimited, where speed unobservability can occur. This new way to evaluate the observer performance makes it also

Manuscript received April 1, 2016; revised June 23, 2016 and September 1, 2016; accepted September 12, 2016.

G. Lefebvre, J-Y. Gauthier, A. Hijazi and X. Lin-Shi are with the Laboratoire Ampère, UMR CNRS 5005, Université de Lyon - INSA Lyon, France (e-mail: xuefang.shi@insa-lyon.fr; jean-yves.gauthier@insa-lyon.fr; alaa.hijazi@insa-lyon.fr).

G. Lefebvre and V. Le Digarcher are with Alstom, Villeurbanne, France (e-mail: gaetan.lefebvre@alstom.com).

possible to avoid the unobservable points to maximise the value of the observability index. Doing so, the performance of observer-based methods are increased. It is the purpose of the Observability-Index Based (OIB) strategy presented in this paper.

The paper is organised as follows. After a call-back of the usual observability study, the AZF method resulting from this study is presented in Section II. In Section III, the observability index is defined. This observability index is used in Section IV to analyse the observer performance. The new control for induction machine sensorless drive is proposed in Section V. Section VI shows the experimental results in order to evaluate the observability index definition relevance and the precision of an observability-index based drive.

II. Induction machine observability study and AZF method

A. Induction machine model

The electrical part of the induction machine is frequently modelled using the stator currents and rotor flux. The usual reference frame is on one hand the rotating reference frame (d, q) for control purpose and, on the other hand, the stationary reference frame (α, β) for observation purpose, since it does not necessitate the preliminary knowledge of the flux position to place the (d) axis. The aim of the present paper being to act on the control references, the (d,q) reference frame will be used. This model is presented in (1), where (i_{sd}, i_{sq}) are the stator currents in the (d,q) reference frame, $(\varphi_{rd}, \varphi_{rq})$ the rotor flux, and ω the electrical speed assumed nearly constant with respect to the currents and flux dynamics. The two controls are the stator voltages (u_{sd}, u_{sq}). R_r and R_s are respectively the rotor and stator resistances, L_r, L_m and L_σ are respectively the rotor, magnetizing and leakage inductances, and ω_s is the frequency of the stator currents. In a sensorless application, the only measured state are the two currents (i_{sd}, i_{sq}), indirectly measured from the phase current measurements.

$$\Sigma_{IM}: \begin{cases} \dot{i}_{sd} = & -\left(\frac{R_s}{L_\sigma} + \frac{L_m^2 R_r}{L_\sigma L_r^2}\right) i_{sd} + \omega_s i_{sq} + \\ & \frac{L_m R_r}{L_\sigma L_r^2}\varphi_{rd} + \frac{L_m \omega}{L_\sigma L_r}\varphi_{rq} + \frac{u_{sd}}{L_\sigma} \\ \dot{i}_{sq} = & -\omega_s i_{sd} - \left(\frac{R_s}{L_\sigma} + \frac{L_m^2 R_r}{L_\sigma L_r^2}\right) i_{sq} - \\ & \frac{L_m \omega}{L_\sigma L_r}\varphi_{rd} + \frac{L_m R_r}{L_\sigma L_r^2}\varphi_{rq} + \frac{u_{sq}}{L_\sigma} \\ \dot{\varphi}_{rd} = & \frac{L_m R_r}{L_r} i_{sd} - \frac{R_r}{L_r}\varphi_{rd} + (\omega_s - \omega)\varphi_{rq} \\ \dot{\varphi}_{rq} = & \frac{L_m R_r}{L_r} i_{sq} - (\omega_s - \omega)\varphi_{rd} - \frac{R_r}{L_r}\varphi_{rq} \\ \dot{\omega} = & 0 \end{cases}$$
$$y = [i_{sd}, i_{sq}] \tag{1}$$

In the (d,q) reference frame, the (d) axis is oriented with the flux. All the flux is given by φ_{rd} and $\varphi_{rq} = 0$. So, it becomes possible to express the slip frequency ω_r (2). The electrical torque T_e is given in (3), where N_p represents the number of pole pairs.

$$\omega_r = \omega_s - \omega = \frac{R_r L_m}{L_r}\frac{i_{sq}}{\varphi_{rd}} \tag{2}$$

$$T_e = \frac{N_p L_m}{L_r}\varphi_{rd} i_{sq} \tag{3}$$

B. Nonlinear observability definition

The observability of nonlinear systems is deduced by the analysis of the rank condition of the observability matrix using Lie derivatives [18]. Considering the nonlinear system Σ (4), the observability matrix of the system, $\mathcal{O}_\Sigma$, is given in (5), where L is the observation space of the system (6).

$$\Sigma: \begin{cases} \dot{x} = f(x,u) \\ y = h(x) \end{cases} \tag{4}$$

$$\mathcal{O}_\Sigma = \frac{\partial L}{\partial x} \tag{5}$$

$$L = \begin{bmatrix} \mathcal{L}_f^0 h \\ \mathcal{L}_f^1 h \\ \vdots \\ \mathcal{L}_f^p h \end{bmatrix} \quad \text{and} \quad \begin{cases} \mathcal{L}_f^0 h = h(x_0) \\ \mathcal{L}_f h = \frac{\partial h}{\partial x} f(x_0) \\ \forall k \in \mathbb{N}^*, \mathcal{L}_f^k = \mathcal{L}_f(\mathcal{L}_f^{k-1} h) \end{cases} \tag{6}$$

If $\mathcal{O}_\Sigma$ is a full rank matrix at x_0 then Σ is said locally weakly observable at x_0.

C. Induction machine observability study

The study of the state vector observability was already presented in diverse ways, with continuous model [5], [19], [20] and discrete-time model [21], for the induction machine in the stationary reference frame (α,β). The observability matrix $\mathcal{O}_{\Sigma_{IM}}$ using the rotating reference frame (d,q) is presented in (7). This observability matrix is obtained by the measurements and theirs two first derivatives. Higher derivation terms would involve flux derivations of second order and more that would not modify the observability analysis [22]. A base change has been done to allow a simpler representation.

$$\mathcal{O}_{\Sigma_{IM}} = \frac{L_m^3}{L_\sigma^3 L_r^2}\begin{bmatrix} 1 & 0 & 0 & 0 & 0 \\ 0 & 1 & 0 & 0 & 0 \\ 0 & 0 & \frac{R_r}{L_r} & \omega & 0 \\ 0 & 0 & -\omega & \frac{R_r}{L_r} & 0 \\ 0 & 0 & 0 & 0 & \omega_s \varphi_{rd} \\ 0 & 0 & 0 & 0 & -\dot{\varphi}_{rd} \end{bmatrix} \tag{7}$$

In constant flux operations, the state vector is observable while the stator frequency ω_s remains non-zero. This is in concordance with the observability conditions presented in the literature [5] even if the reference frame changed.

From (2) and (3), the stator frequency variation with the electrical torque is expressed in (8).

$$\omega_s = \omega + \omega_r = \omega + \frac{R_r}{N_p}\frac{T_e}{\varphi_{rd}^2} \tag{8}$$

Therefore, the unobservable points can be expressed in the (T_e, ω) plane as a line named unobservability line [19], described by (9) and shown in Fig. 1. A delicate area for speed observation is defined as the speed range where the stator frequency can take zero value depending on the electrical torque. It is a simple way to know whether unobservable conditions can occur in a given application.

$$T_e = -\frac{N_p \varphi_{rd}^2}{R_r}\omega \tag{9}$$

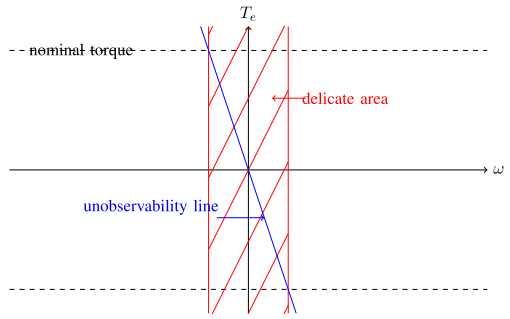

Fig. 1. Unobservability line in the (ω, T_e) plane with a constant flux.

D. Method to avoid zero-frequency operation

The unobservable points have been pointed out. In [16], [17] and more recently in [23], it has been proposed to define a zone to avoid, between two stator-frequency values, $\pm\omega_s^{lim}$. This control modification is the purpose of the AZF method. The modification of the stator frequency is performed through a modification of the flux amplitude. The torque and the speed stay unchanged while the stator-frequency is controlled.

From this principle, our paper will explain how the AZF method improves the observability. The minimum stator frequency defined by the user is w_s^{lim}. $T_e^{\#}$ and $\varphi_{rd}^{\prime\#}$ are the torque and flux references. Using (8), the flux modification is done as reported in (10). It occurs only when $|\omega_s| \leq \omega_s^{lim}$.

$$\varphi_{rd}^{\prime\#} = \begin{cases} \sqrt{\frac{T_e^{\#} R_r}{N_p(\omega_s^{lim} - \omega)}} & \text{if } T_e^{\#} \geq 0 \\ \sqrt{\frac{T_e^{\#} R_r}{N_p(-\omega_s^{lim} - \omega)}} & \text{if } T_e^{\#} < 0 \end{cases} \tag{10}$$

With the diagram of a classical field-oriented control implementation (Fig. 2.a), this flux modification is performed here as described in Fig. 2.b. A flux regulator is introduced in order to have a quick flux variation. Since the flux is varying, the torque is no longer regulated through the I_q regulation. So, the I_q reference is adapted depending on the flux estimation.

Thanks to the results from the observability study, the AZF method can be interpreted as an avoidance of the points where the observability is zero. This analysis is yet limited to a binary knowledge: whether the system is observable or not. Thereafter, an observability index that evaluates continuously the observability will be introduced.

III. Observability index: definition

A. Observability continuous evaluation

The problem of a continuous evaluation of the observability was first tackled for linear systems [24] using the observability matrix [25]. In the paper [26] was proposed three observability indexes from the observability matrix, and three others from the observability gramian. Among the six indexes proposed for a linear system, each one can give a different part of the information. The observability of the least observable state is given by the minimum eigenvalue of the observability matrix or gramian. A mean observability of the system is given by the determinant and trace of the observability matrix or gramian. It appears that none can be seen as the best observability index.

For nonlinear systems, a similar definition is more complicated to find and to prove. The definitions found in the literature mainly use the observability matrix [22], [27] or the empirical observability gramian [28], [29]. The empirical observability gramian, defined in [30], provides a numeric value of the observability and is only relevant for a given point or trajectory. For its part, the observability matrix provides an analytic value that remains relevant for all points or trajectories. So, the observability matrix is chosen to define the observability index in this paper.

As for linear systems, once the observability matrix is chosen to define the observability index, three criteria can be used: the minimum eigenvalue, the trace and the determinant of the product of the observability matrix with its transpose. The similar need to reduce the information contained in a matrix to a scalar number exists for identification problems using the sensibility matrix [31]. In [32], the use of the determinant of the matrix is presented as the most significant since it considers the confidence in the observation of the global system, considering the errors committed on each state weighted by the sensitivity of the observation to this given state. This criterion is also invariant with rescaling transformation and it is the most commonly used.

Consequently, the continuous observability index of the system Σ, noted η_Σ, is defined by (11). The larger this value is, the better the observability will be.

$$\eta_\Sigma = \det(\mathcal{O}_\Sigma^T \mathcal{O}_\Sigma) \tag{11}$$

B. Observability index application to induction machine

Using definition of (11) and the observability matrix from (7), the observability index of a sensorless induction machine, $\eta_{\Sigma_{IM}}$, is presented in (12).

$$\eta_{\Sigma_{IM}} = \left(\frac{L_m^3}{L_\sigma^3 L_r^2}\right)^2 \left(\left(\frac{R_r}{L_r}\right)^2 + \omega^2\right)^2 \left(\left(\omega_s \varphi_{rd}\right)^2 + \dot{\varphi}_{rd}^2\right)^2 \tag{12}$$

The flux φ_{rd} is generally a constant value, and the speed is set by the use conditions. So, the observability index can be reduced to a value η_1 defined in (13) that represents the same observability information as (12), but is easier to calculate. This value will be used for the rest of the paper.

$$\eta_1 = \left(\omega_s \varphi_{rd}\right)^2 \tag{13}$$

IV. Observability index: analysis

A. Observability index analysis for a classical control

The observability index can be expressed, using (8), as a function varying with the flux φ_{rd}, the torque, and the speed, as expressed in (14). It gives the possibility to analyse the induction machine observability index depending on these values. The machine used for this study is a 1.5 kW induction machine whose parameters are presented in Table I.

$$\eta_1 = \left(\omega \varphi_{rd} + \frac{R_r}{N_p} \frac{T_e}{\varphi_{rd}}\right)^2 \tag{14}$$

The definition of the observability index enables the analysis of the observability of an induction machine in a sensorless

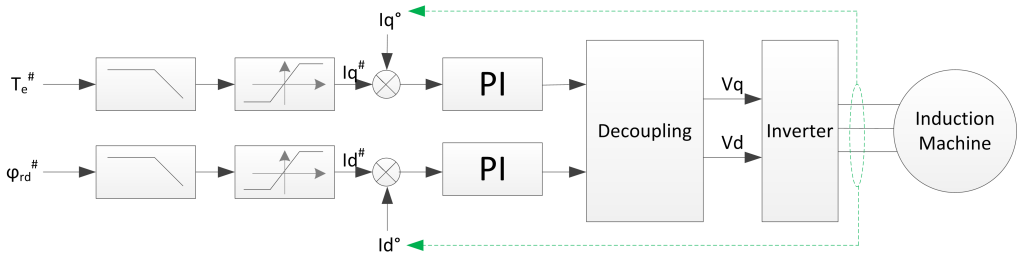

(a) Classical field-oriented control.

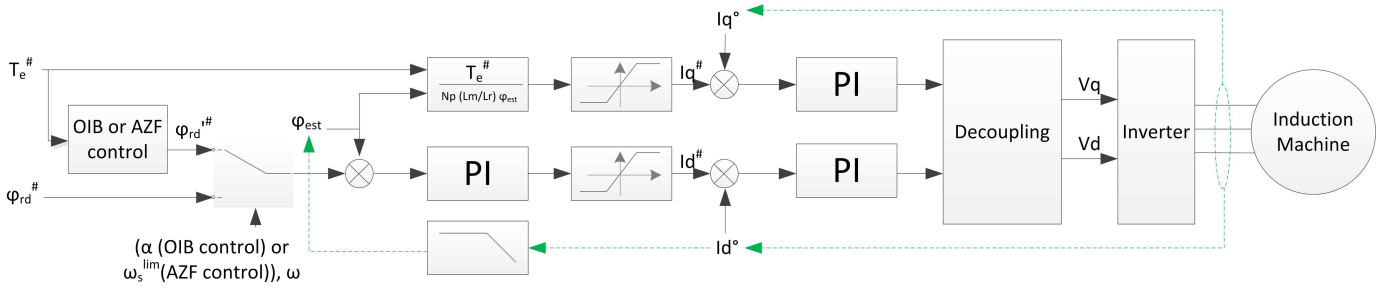

(b) Field-oriented control adapted for AZF or OIB control strategy.

Fig. 2. Adaptation of a field-oriented control to be used with an AZF or OIB control strategy.

TABLE I
INDUCTION MACHINE PARAMETERS.

Electrical parameters		
N_p	number of poles pair	2
R_r	rotor resistance	1.89 Ω
R_s	stator resistance	4.61 Ω
L_m	magnetizing inductance	602 mH
L_σ	leakage inductance	75 mH
Nominal values		
P_{nom}	nominal power	1.5 kW
I_{nom}	nominal current	3.1 A
V_{nom}	nominal voltage	400 V
φ_{nom}	nominal flux	0.81 Wb
Ω_{nom}	nominal speed	1455 rpm
$T_{e\,nom}$	nominal torque	9.4 Nm

application. To start with, the case of a classical field-oriented control is considered. The flux remains constant at its nominal value. The observability index η_1 is presented in Fig. 3. Only the low-speed operating points are studied, since they are the most challenging. The electrical speed range considered is thus between -100 and 100 rpm, while the whole torque range is considered. The observability index variations higher than $20\,\mathrm{Wb}^2{\cdot}\mathrm{rad}^2{\cdot}\mathrm{s}^{-2}$ have not been represented. The unobservability line can be seen considering the zero-observability-index points. The observability index map also provides information on the behaviour around this unobservability line.

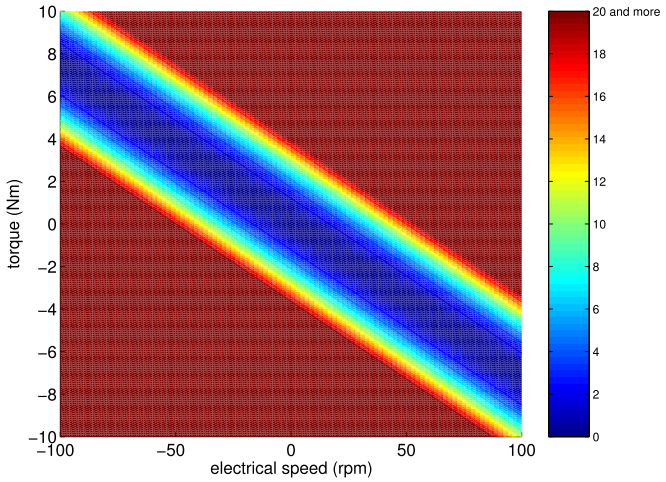

Fig. 3. Observability index η_1 using a classical control.

B. Observability index analysis for the AZF method

The same analysis can be done in the case of a control using the AZF method. The flux is modified depending on the torque and speed, using the flux reference modification reported in (10). The flux amplitude is however limited, between a maximum value due to the machine design and a minimum value in order not to demagnetize the machine. The maximum value is usually the nominal flux, φ_{nom}. The minimum value, φ_{min}, is set here to a quarter of the nominal flux. Using these flux values, the observability index is plotted with respect to the speed and the torque in Fig. 4. The stator-frequency limit value, ω_s^{lim}, has been set to 1 Hz.

The observability index is globally increased using the AZF method but this increase is not uniform. The observability index is highly increased for high-torque operation, while the impact for low-torque operation is less important. It is even reduced around zero-torque.

Actually, the criteria on which the control is defined, the stator frequency ω_s, only describes one part of the observability index η_1 defined in (13). By maximizing the stator frequency, the flux can be reduced so that the observability index is finally decreased. This analysis shows that the observability index is a tool to analyse the observability that explains clearly the limitation of the AZF method. A new control strategy, based

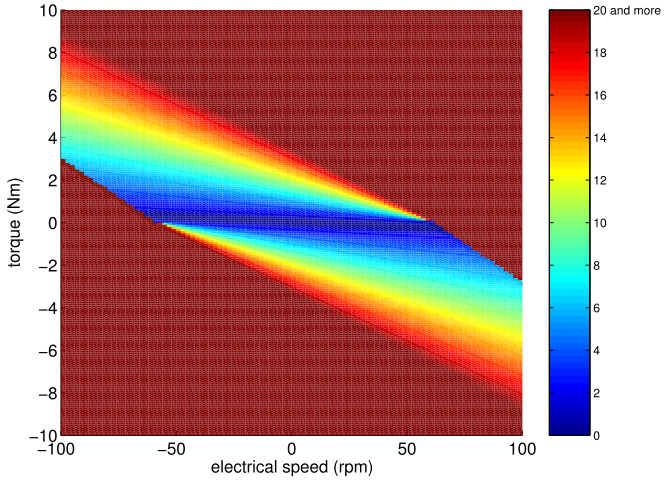

Fig. 4. Observability index η_1 witn a control using an AZF method.

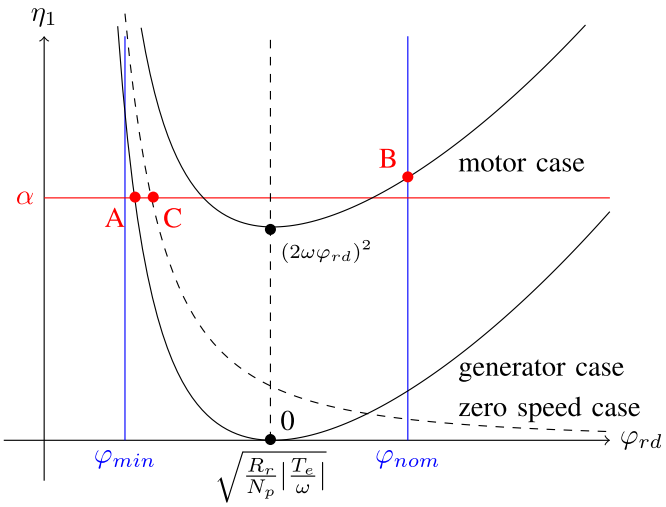

Fig. 5. Unobservability index variations with respect to the flux.

on the observability index, is thus proposed.

V. Observability-index based control strategy

A. Control strategy presentation

The observability index has been presented in (14) as a function varying with the flux φ_{rd}. By modifying this flux, the observability index can be modified while the speed and the torque stay unchanged. The purpose of the observability-index based (OIB) strategy is to get an observability index higher than a given value α by modifying the flux reference without modifying the electrical torque T_e, the most important value to control. Doing so, the control is not modified while the speed observability is increased. It corresponds to solving an inequality under flux constraints (15).

$$\begin{cases} \eta_1(\varphi_{rd}) \geq \alpha \\ \varphi_{min} \geq \varphi_{rd} \geq \varphi_{nom} \end{cases} \tag{15}$$

Fig. 5 presents the observability index variation with respect to the flux. Three cases can be considered, whether the machine is used in motor or in generator condition, and a third case for zero speed operation (dashed line). These are the three typical curves that can be encountered. When the machine is used as a motor, the minimum observability index is always a positive value. When the machine is used as a generator, the minimum observability index is always zero.

In the operating conditions presented as an example on Fig. 5, in the generator case, the flux will be modified to reach point A in order to ensure the observability of the speed. In motor case, the observability index for nominal flux, point B, is higher than the limit value α, the flux reference is not modified. In zero speed case, the flux will be modified to reach point C where the observability index is equal to α. If the whole flux range leads to an observability index lower than α, the flux providing the maximum observability index is used as the reference.

The resolution of the equation $\eta_1(\varphi_{rd}) = \alpha$ leads to two solutions, φ_1 and φ_2, given in (16). The flux reference selection is done according to the algorithm presented in Fig. 6.

$$\begin{cases} \begin{cases} \varphi_1 = \left|\frac{\sqrt{\alpha}-\sqrt{\Delta}}{2\omega}\right| \\ \varphi_2 = \left|\frac{\sqrt{\alpha}+\sqrt{\Delta}}{2\omega}\right| \\ \Delta = \alpha - 4\omega\frac{R_r}{N_p}T_e^{\#} \end{cases} & \text{if } \omega \neq 0 \\ \varphi_1 = \varphi_2 = \frac{R_r}{N_p}\frac{|T_e^{\#}|}{\sqrt{\alpha}} & \text{if } \omega = 0 \end{cases} \tag{16}$$

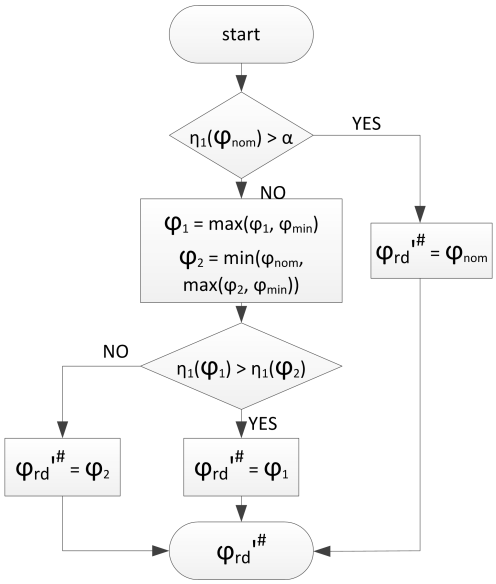

Fig. 6. Algorithm of the observability-based control strategy.

The implementation of the observability-index based control strategy is done in the same way as presented on Fig. 2.

B. Observability analysis using the OIB strategy

To show the effectiveness of the proposed control, the OIB strategy is analysed in the same way as that described in Section IV. Fig. 7 presents the observability index variations in the (ω, T_e) plane with the observability index limit, α, set to 16 $\mathrm{Wb^2{\cdot}rad^2{\cdot}s^{-2}}$. It appears that for most of the low-observability-index working points, the observability index

value has been increased to reach the limit value α. For low-torque and low-speed operating points, the flux variation is limited by the flux minimum value, and the observability index gets values lower than α. It can be foreseen that in such conditions, the observation performance will remain poor.

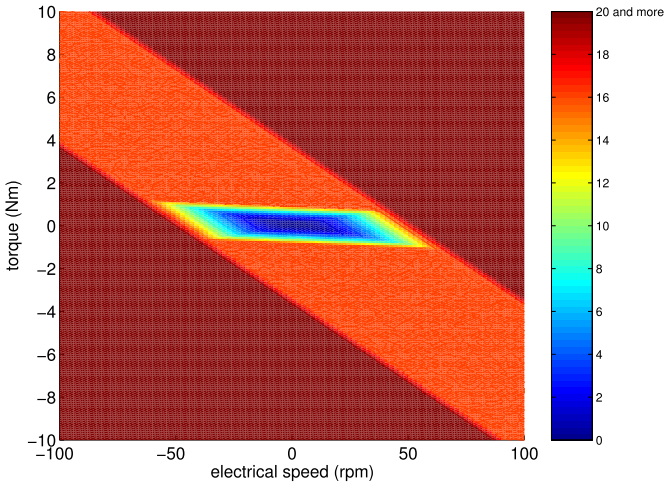

Fig. 7. Observability index η_1 using an OIB control strategy.

C. Comparison of AZF and OIB control strategies

The comparison between the observability index using the AZF (Fig. 4) and the OIB (Fig. 7) control strategy shows that they both globally increase the observability index. Thus, they are both suitable to improve the speed observation performance. Meanwhile, the OIB strategy increases this index on a wider range. For low-torque operation, it even provides a largely better observability index. This point is independent of both control strategies tunings since the AZF method leads to a continuous variation of the index, while the OIB strategy generates a constant observability index, except for the low-speed and low-torque operating points. An other positive point of the OIB strategy is that it provides a uniform observability index, which makes the tuning of this strategy easier.

VI. Experimental results

A. Experiment environment

To demonstrate the pertinence of the observability index analysis and of the OIB strategy, an experimental motor test-bench has been used. The test-bench is shown in Fig. 8. It is composed of one 1.5 kW induction machine whose parameters are presented in Table I coupled to a 1.7 kW permanent magnet synchronous machine (PMSM) whose parameters are presented in Table II.

The PMSM is driven by an industrial inverter. The induction machine is driven by an inverter composed of IGBT and the control is implemented on a dSPACE prototyping system. The three currents are measured using fluxgate sensors. The DC voltage of the inverter is measured and used for the pulse width modulation. The speed observer is an extended Kalman filter augmented to the load torque, similar to the one presented in [33] except that the equations are here normalised. It works in the (α,β) reference frame. The observer is not modified from an experiment to the other and its tunings stay unchanged. The call frequency of both the control and the observer is set to 1 kHz. The PWM switching frequency is set to 10 kHz.

TABLE II
Permanent magnet synchronous machine parameters.

Electrical parameters		
N_p	number of poles pair	3
R_s	stator resistance	2.3 Ω
L_s	magnetizing inductance	8,9 mH
Nominal values		
P_{nom}	nominal power	1.7 kW
I_{nom}	nominal current	3.81 A
V_{nom}	nominal voltage	750 V
Ω_{nom}	nominal speed	3000 rpm
$T_{e\,nom}$	nominal torque	5.4 Nm

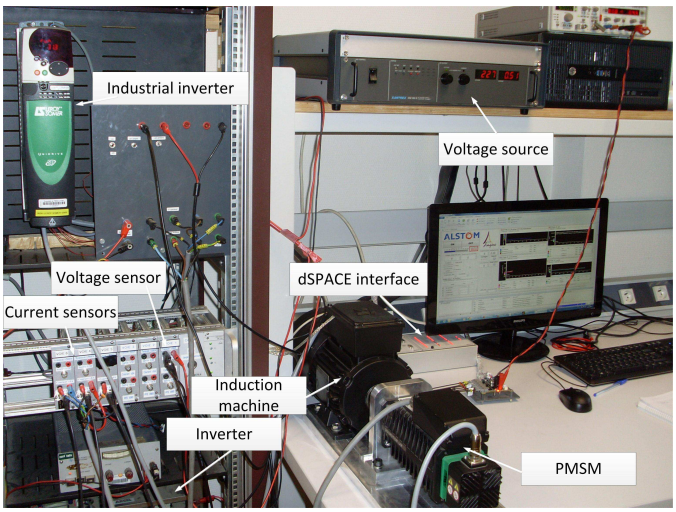

Fig. 8. Motor test-bench used for the experiment.

B. Test profile definition

The test profile of this experiment is defined for two purposes: evaluating the pertinence of the observability index η_1 and evaluating the improvements of the speed observer performance given by the use of the OIB control strategy compared with the AZF method. The test profile is presented in the (ω, T_e) plane in Fig. 9 over the observability index when an AZF method is used. It crosses twice the unobservability line, once with a high torque reference (from point A to point B), and the second time with a low torque reference (from point C to point D). The whole profile follows regenerative braking conditions. Since the purpose of this paper is to evaluate the speed observer performance for long time operation close to unobservable conditions, the time operation between each point is chosen at 30 s. Especially, the operation from point D to point A corresponds to a long in load speed evolution from 20 electrical rpm (0.33 Hz or 2.1 rad·s^{-1}) to zero speed. The PMSM maximum torque being lower than the induction machine maximum torque, the high torque reference is set to 5.4 Nm. The low torque reference is set to 1 Nm.

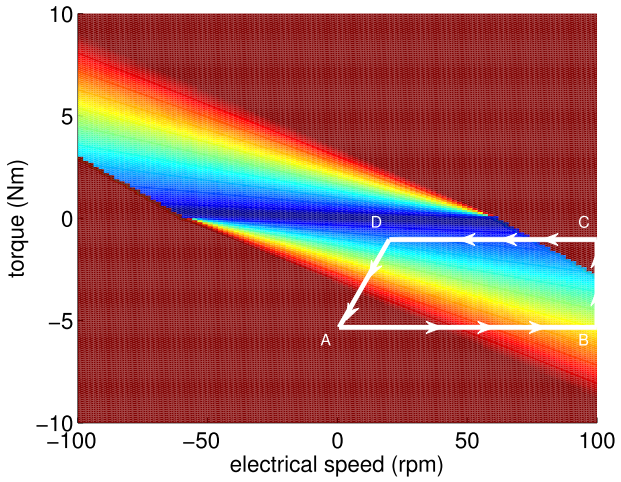

Fig. 9. Test profile used for the experiments.

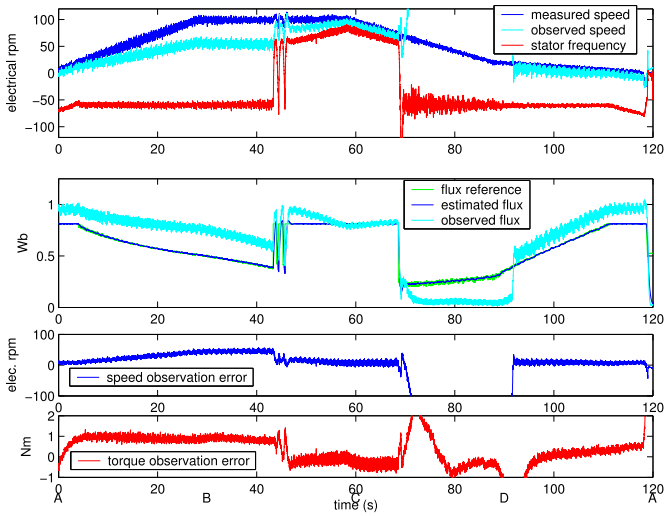

Fig. 11. Experimental result with an AZF method.

C. Classical control vs. AZF method

First, the observed speed is not used for the control in order to evaluate the speed observation error. The profile defined is used with a classical field-oriented control and then with an AZF method with a stator frequency limit set to $\omega_s^{lim} = 1\,\text{Hz}$. The results are presented for the classical vector control in Fig. 10 and for the AZF method in Fig. 11.

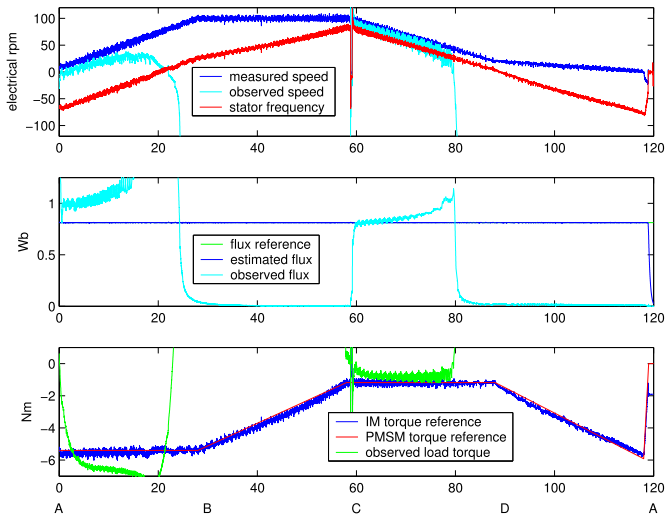

Fig. 10. Experimental result with a classical field-oriented control.

When a classical field-oriented control is used, the speed observer diverges twice, each time the low-observability area is crossed. Because of this divergence, the speed observer has been re-initialized at $t = 60\,\text{s}$ so that the speed observation could be studied in the remaining part of the experiment. On the first crossing of the low-observability area, at high-torque, the AZF method ensures a sufficient observability so that the speed observer remains precise. It shows the interest of the AZF method that enables to make the speed observer work on a wider range of the (ω, T_e) plane. On the second crossing, at low torque, the same method leads to a divergence of the speed observation. The observability index on this point is actually low, even if the stator frequency remains at its limit value ω_s^{lim}. The speed observation converges once again as soon as the observability index gets back to a sufficient value.

This experiment shows that, despite its characteristics for high torque operation, the AZF method is not adapted for low torque operation. But the most important point to notice is that this low-performance was foreseen by the observability index analysis. The observability index is a reliable tool to forecast the performance of the observer.

D. AZF vs. OIB control strategy

The effectiveness of the observability index analysis has been proved with the experiment, and the poor results of the AZF method for low-torque operation has been shown. Here, the OIB strategy with $\alpha = 16\,\text{Wb}^2\cdot\text{rad}^2\cdot\text{s}^{-2}$ is implemented on the same profile, using the same observer with the same tunings. Fig. 12 presents the results of this experiment.

The speed observation is now converging in every condition. It underlines once more the correlation between the observability index value and the observer precision.

Table III compares the RMS speed observation error and current consumption between various tunings of the AZF method and the proposed OIB control strategy. It points out that, for a similar current consumption, the speed observer error with the OIB strategy is always lower than the one using an AZF method. This improvement is independent of the control parameter tunings, ω_s^{lim} or α. The observer performance depend on the value α chosen in the OIB strategy. The value α can thus be tuned according to the speed observer performance expectation and the flux deviation achievable.

E. Closed-loop experiment

The observed speed is now used in the control. The control and the observer work in closed loop. The OIB control strategy is used. This is an effective induction machine sensorless drive performed on the same test profile whose results are

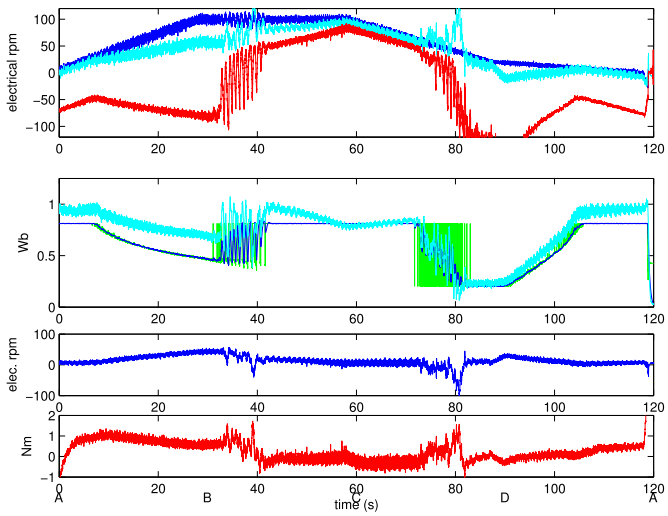

Fig. 12. Experimental result with an OIB control strategy. Explanation of curves are as in Fig. 11.

TABLE III
RESULTS WITH VARIOUS TUNINGS OF THE AZF AND OIB STRATEGIES.

ω_s^{lim} (Hz)	1/3	1/2	1	1.5	2
RMS speed observation error (rpm)	4364	178	116	73	69
RMS current consumption (A)	3.8	3.85	4.2	4.7	5.0
α ($\mathrm{Wb}^2{\cdot}\mathrm{rad}^2{\cdot}\mathrm{s}^{-2}$)	4	9	16	25	36
RMS speed observation error (rpm)	5525	6159	25	33	43
RMS current consumption (A)	3.8	4.0	4.2	4.5	5.0

presented in Fig. 13. Because of the instabilities generated by the loop closure, the minimum observability index is increased from 16 to $20\,\mathrm{Wb}^2{\cdot}\mathrm{rad}^2{\cdot}\mathrm{s}^{-2}$. The experiment results on this challenging test profile proves that the OIB strategy is an adequate solution for induction machine sensorless drive.

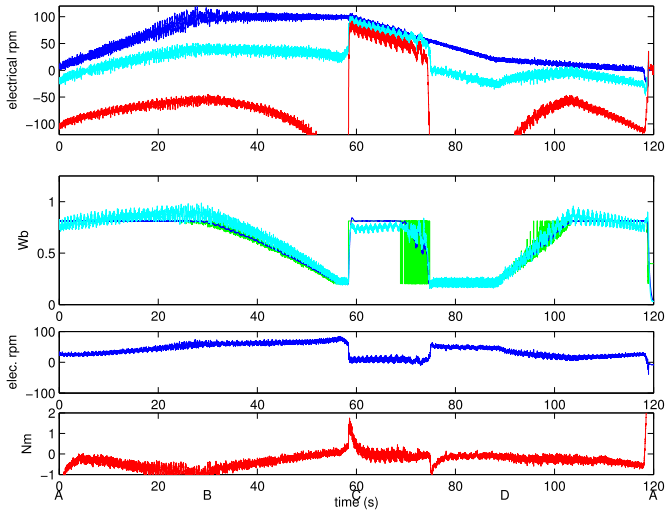

Fig. 13. Sensorless drive using the OIB control strategy. Explanation of curves are as in Fig. 11.

VII. CONCLUSION

In this paper, the observability study of the induction machine sensorless drive has been performed with a continuous evaluation of the observability. To do so, an observability index has been defined. The pertinence of this observability index was shown by linking the observability index with the speed observation performance. To start with, an existing method has been studied and its limits have been pointed out using the observability index analysis. Then, the observability-index based control strategy has been proposed. It improves induction machine sensorless drive solutions that do not necessitate any signal injection. The experimentations both in open loop and closed loop showed the improvements. It also demonstrates that the observability-index based control strategy offers a new path for induction machine sensorless drives without signal injection. Using a Kalman filter, the observability-index based control strategy notably improved the speed sensorless operation in the neighbourhood of unobservable conditions. The use of any more efficient observer, the consideration of the inverter non linearities or the joint observation of electrical parameters would even more improve the induction machine speed sensorless drive. It is a perspective for this work.

REFERENCES

[1] C. Schauder, "Adaptive speed identification for vector control of induction motors without rotational transducers," *IEEE Transactions on Industry Applications*, vol. 28, DOI 10.1109/28.158829, no. 5, pp. 1054–1061, Sep. 1992.

[2] Y.-R. Kim, S.-K. Sul, and M.-H. Park, "Speed sensorless vector control of induction motor using extended kalman filter," *IEEE Transactions on Industry Applications*, vol. 30, DOI 10.1109/28.315233, no. 5, pp. 1225–1233, Sep. 1994.

[3] T. Du, P. Vas, and F. Stronach, "Design and application of extended observers for joint state and parameter estimation in high-performance ac drives," *IEE Proceedings - Electric Power Applications*, vol. 142, DOI 10.1049/ip-epa:19951701, pp. 71–78, Mar. 1995.

[4] J. Holtz, "Sensorless control of induction machines - with or without signal injection?" *IEEE Transactions on Industrial Electronics*, vol. 53, DOI 10.1109/TIE.2005.862324, no. 1, pp. 7–30, Feb. 2006.

[5] P. Vaclavek, P. Blaha, and I. Herman, "Ac drive observability analysis," *IEEE Transactions on Industrial Electronics*, vol. 60, DOI 10.1109/TIE.2012.2203775, no. 8, pp. 3047–3059, Aug. 2013.

[6] S. Suwankawin and S. Sangwongwanich, "Design strategy of an adaptive full-order observer for speed-sensorless induction-motor drives-tracking performance and stabilization," *IEEE Transactions on Industrial Electronics*, vol. 53, DOI 10.1109/TIE.2005.862308, no. 1, pp. 96–119, Feb. 2005.

[7] W. Sun, J. Gao, Y. Yu, G. Wang, and D. Xu, "Robustness improvement of speed estimation in speed sensorless induction motor drives," *IEEE Transactions on Industry Applications*, vol. 52, DOI 10.1109/TIA.2015.2512531, no. 3, pp. 2525–2536, May. 2016.

[8] M. Schroedl, "Sensorless control of ac machines at low speed and standstill based on the ldquo;inform rdquo; method," in *Industry Applications Conference., Conference Record of the 1996 IEEE*, vol. 1, DOI 10.1109/IAS.1996.557028, Oct. 1996, pp. 270–277 vol.1.

[9] J.-I. Ha and S.-K. Sul, "Sensorless field-orientation control of an induction machine by high-frequency signal injection," *IEEE Transactions on Industry Applications*, vol. 35, DOI 10.1109/28.740844, no. 1, pp. 45–51, Jan. 1999.

[10] S. Nandi, S. Ahmed, H. A. Toliyat, and R. M. Bharadwaj, "Selection criteria of induction machines for speed-sensorless drive applications," *IEEE Transactions on Industry Applications*, vol. 39, DOI 10.1109/TIA.2003.810651, no. 3, pp. 704–712, May. 2003.

[11] C. Caruana, G. M. Asher, and M. Sumner, "Performance of hf signal injection techniques for zero-low-frequency vector control of induction machines under sensorless conditions," *IEEE Transactions on Industrial Electronics*, vol. 53, DOI 10.1109/TIE.2005.862257, no. 1, pp. 225–238, Feb. 2006.

[12] H. Zatocil, "Sensorless control of induction motor drives in the zero frequency speed range," in *Power Electronics and Applications. 13th European Conference on*, Sep. 2009, pp. 1–10.

[13] S. Kim and S. K. Sul, "Sensorless control of ac motor - where are we now?" in *Electrical Machines and Systems (ICEMS), 2011 International Conference on*, DOI 10.1109/ICEMS.2011.6073316, 2011, pp. 1–6.

[14] V.-M. Leppänen and J. Luomi, "Speed-sensorless induction machine control for zero speed and frequency," *IEEE Transactions on Industrial Electronics*, vol. 51, DOI 10.1109/TIE.2004.834965, pp. 1041–1047, Oct. 2004.

[15] D. Basic, F. Malrait, and P. Rouchon, "Current controller for low-frequency signal injection and rotor flux position tracking at low speeds," *IEEE Transactions on Industrial Electronics*, vol. 58, DOI 10.1109/TIE.2010.2100336, no. 9, pp. 4010–4022, Sep. 2011.

[16] M. Depenbrock, C. Foerth, and S. Koch, "Speed sensorless control of induction motors at very low stator frequencies," in *EPE '99*, 1999.

[17] H. Kubota, I. Sato, Y. Tamura, K. Matsuse, H. Ohta, and Y. Hori, "Regenerating-mode low-speed operation of sensorless induction motor drive with adaptive observer," *IEEE Transactions on Industry Applications*, vol. 38, DOI 10.1109/TIA.2002.800575, no. 4, pp. 1081–1086, Jul. 2002.

[18] R. Hermann and A. Krener, "Nonlinear controllability and observability," *IEEE Transactions on Automatic Control*, vol. 22, DOI 10.1109/TAC.1977.1101601, no. 5, pp. 728–740, Oct. 1977.

[19] C. Canudas De Wit, A. Youssef, J. P. Barbot, P. Martin, and F. Malrait, "Observability conditions of induction motors at low frequencies," in *Decision and Control, 2000. Proceedings of the 39th IEEE Conference on*, vol. 3, DOI 10.1109/CDC.2000.914093, 2000, pp. 2044–2049 vol.3.

[20] M. Koteich, A. Maloum, G. Duc, and G. Sandou, "Discussion on "ac drive observability analysis"," *IEEE Transactions on Industrial Electronics*, vol. 62, DOI 10.1109/TIE.2015.2438777, no. 11, pp. 7224–7225, Nov. 2015.

[21] F. Alonge, T. Cangemi, F. D'Ippolito, A. Fagiolini, and A. Sferlazza, "Convergence analysis of extended kalman filter for sensorless control of induction motor," *IEEE Transactions on Industrial Electronics*, vol. 62, DOI 10.1109/TIE.2014.2355133, no. 4, pp. 2341–2352, Apr. 2015.

[22] M. Ghanes, J. D. Leon, and A. Glumineau, "Observability study and observer-based interconnected form for sensorless induction motor," in *Decision and Control, 2006 45th IEEE Conference on*, DOI 10.1109/CDC.2006.376711, Dec. 2006, pp. 1240–1245.

[23] G. Lefebvre, V. Le Digarcher, J.-Y. Gauthier, A. Hijazi, and X. Lin-Shi, "Optimal low-stator-frequency avoidance strategy to improve the performances of induction machines sensorless drives," in *Sensorless Control for Electrical Drives (SLED), 2015 IEEE Symposium on*, DOI 10.1109/SLED.2015.7339256, Jun. 2015, pp. 1–6.

[24] H. L. Ablin, "Criteria for degree of observability in a control system," Ph.D. dissertation, Iowa State University, 1967.

[25] R. Kalman, "On the general theory of control systems," *IRE Transactions on Automatic Control*, vol. 4, DOI 10.1109/TAC.1959.1104873, no. 3, Dec. 1959.

[26] P. Müller and H. Weber, "Analysis and optimization of certain qualities of controllability and observability for linear dynamical systems," *Automatica*, vol. 8, DOI 10.1016/0005-1098(72)90044-1, no. 3, pp. 237–246, 1972.

[27] C. Böhm, R. Findeisen, and F. Allgöwer, "Avoidance of poorly observable trajectories: A predictive control perspective," in *Proceedings of the 17th IFAC World Congress*, DOI 10.3182/20080706-5-KR-1001.00332, 2008, pp. 1952–1957.

[28] A. J. Krener and K. Ide, "Measures of unobservability," in *Decision and Control, Proceedings of the 48th IEEE Conference on*, DOI 10.1109/CDC.2009.5400067, Dec. 2009, pp. 6401–6406.

[29] A. K. Singh and J. Hahn, "Sensor location for stable nonlinear dynamic systems : Multiple sensor case," *Industrial & Engineering Chemistry Research*, vol. 45, DOI 10.1021/ie0511175, pp. 3615–3623, 2006.

[30] S. Lall, J. E. Marsden, and S. Glavaski, "A subspace approach to balanced truncation for model reduction of nonlinear control systems," *International Journal on Robust and Nonlinear Control*, vol. 12, DOI 10.1002/rnc.657, pp. 519–535, 2002.

[31] J. Qian, M. Nadri, P.-D. Morosan, and P. Dufour, "Closed loop optimal experiment design for on-line parameter estimation," in *Control Conference (ECC), 2014 European*, DOI 10.1109/ECC.2014.6862468, Jun. 2014, pp. 1813–1818.

[32] G. Franceschini and S. Macchietto, "Model-based design of experiments for parameter precision: State of the art," *Chemical Engineering Science*, vol. 63, DOI 10.1016/j.ces.2007.11.034, no. 19, pp. 4846–4872, 2008.

[33] M. Barut, S. Bogosyan, and M. Gokasan, "Speed-sensorless estimation for induction motors using extended kalman filters," *IEEE Transactions on Industrial Electronics*, vol. 54, DOI 10.1109/TIE.2006.885123, no. 1, pp. 272–280, Feb. 2007.

Gaëtan Lefebvre received, in 2013, the Diploma of engineer (M.Eng.) from Ecole Supérieur d'Electricité, Gif-sur-Yvette, France, and the M.Sc. degree in information, energy and system from Université de Paris-Saclay, France.

In 2013, he joined both the Ampère Laboratory in Lyon, France and Alstom in Villeurbanne, France for his Ph.D, to work on railway traction motor drives. His research interests concerns design, control and observation of electrical and mechanical systems for transportation applications.

Jean-Yves Gauthier received the Graduate degree in electrical engineering from Ecole Normale Supérieure, Cachan, France, in 2003 and the DEA (M.Sc.) degree in applied informatics and automation and the Ph.D. degree both from the University of Franche-Comté, France, in 2004 and 2007, respectively.

His Ph.D. research fields were about the modeling and the control of magnetic shape memory alloy-based actuators. In 2008, he became an Associate Professor at INSA Lyon, Villeurbanne, France, working at the Laboratoire de Génie Electrique et de Ferroélectricité in semiactive vibration control using piezoelectric devices. Since 2012, he has been working at Ampère Lab, Villeurbanne, France. His current research interests include the control of power electronic devices and electrical motor drives.

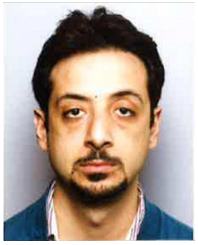

Alaa Hijazi was born in Blida, South Lebanon, in 1983. In 2010, he received the Ph.D. degree in electrical engineering from the Lyon 1 University, France.

In 2011, he joined the INSA (National Institutes of Applied Sciences) of Lyon School of engineering as Assistant Professor at Ampère laboratory. His research interests concerns control and observation of electrical systems.

Xuefang Lin-Shi received the Ph.D degree in applied computer science and automatic in 1992 from INSA Lyon (Institut National des Sciences Appliquées de Lyon), France.

Since 1993, she has been with the Electrical Engineering department of INSA Lyon, where she is currently a professor. She is now with Ampère Laboratory in Lyon. Her research interests concern control applied to electrical drives and power electronics system.

Vincent Le Digarcher received the Diploma of engineer (M.Eng.) from Ecole supérieure de chimie, physique, électronique de Lyon, Villeurbanne, France, in 2006.

From 2004 to 2005, he spent one year as research assistant in biomedical engineering at University of North Carolina. In 2006, he joined Alstom, Villeurbanne, France to work on railway traction motor drives. Since 2015, he is with Alstom in Sydney, Australia.